CONTROL OF THREE-DIMENSIONAL SEPARATION ON HIGHLY-SWEPT WINGS

P R Ashill, G L Riddle and M J Stanley
Defence Research Agency, Bedford, England MK41 6AE

Summary

The flow over a cambered delta wing of 60° leading-edge sweep is shown to separate from the upper surface at conditions typical of low-speed manoeuvre. For a range of angles of incidence this separation intersects the leading edge and hence provides a route for boundary-layer air to migrate towards the wing leading edge, inducing leading-edge separation. This paper describes wind-tunnel studies of miniature vortex generators to control this flow and so to inhibit leading-edge separation. After describing flows over the basic wing and in the near field of a vortex generator, the paper considers the factors affecting the performance of the vortex generators, including angle of incidence, position, geometry and number. It is shown that a vortex generator controls leading-edge separation so long as it is upstream of the upper-surface separation. Increasing the number of vortex generators is beneficial until the vortices are close enough to one another to interfere destructively. It is concluded that vortex generators reduce the extent of leading-edge separation, thus increasing leading-edge thrust and reducing lift dependent drag over a range of angles of incidence.

Notation

A	Wing aspect ratio
C_D	overall drag coefficient
C_{D0}	zero-lift drag coefficient
C_L	overall lift coefficient
C_m	pitching-moment coefficient, about reference point shown in Fig 2a
C_m'	reduced pitching moment coefficient, Figs 5c and 17c
C_p	static pressure coefficient
C_x, C_z	axial (positive downstream) and normal (positive in lift direction) force coefficients
c_0	wing centre-line chord (Fig 2a)
c	geometric mean chord
d	vortex generator diameter
K	lift-dependent drag factor
n	number of vortex generators
P	point on wing leading edge where flow changes from attached to separated
R, R_1, R_2	reattachment lines
S_1, S_2, S_3	separation lines
u_τ	wall friction velocity, $= \sqrt{(\tau_w/\rho)}$ just upstream of VG
S, s	wing planform area and wing semi-span (Fig 2a)
x,y,z	cartesian coordinates with respect to centre-line chord, origin at virtual apex of wing (Fig 2a)
x_p	axial position of point P referred to c_0
x_w, x_{w1}	axial stations defining positions of vortex generators referred to c_0 (Fig 3)
α	angle of incidence
δ^*	boundary-layer displacement thickness just upstream of VG
δx_w	axial distance between vortex generators referred to c_0 (Fig 3)
Δ	increment due to vortex generator(s)
ϕ	angle between VG axis and wing leading edge in plan view (Fig 3)
η	non-dimensional spanwise position, = y/s
τ_w	wall shear stress

Introduction

The design of swept wings for supersonic aircraft is a compromise between the conflicting requirements of efficient supersonic flight and satisfactory performance at subsonic speeds. Similarly, wings for stealthy combat aircraft are a compromise between the requirements of low radar cross-section and good subsonic manoeuvre performance. In both cases, design studies favour wings of relatively-high sweep.

For subsonic manoeuvre at high angles of incidence, flows over highly-swept wings separate on the upper surface. This separation occurs at an envelope of the limiting streamlines, known as an 'ordinary' or three-dimensional separation line[1]. Faced with the problem of maintaining attached flow on wings of this type in the 1950's, Küchemann[2] suggested that the flow should be forced to separate cleanly from an aerodynamically-sharp leading edge to form an orderly vortex sheet. This type of flow is exploited in the design of Concorde to achieve the required take-off and landing performance. Küchemann argued that this class of flow avoids 'undesirable trim changes' of wings where separation is not fixed along the whole length of the leading edge. Unfortunately, planar wings with leading edge separation have high lift-dependent drag factors, typically 2.5 for a 60° delta wing. Wings with such a high lift-dependent drag factor are probably unsuitable for combat aircraft designed to manoeuvre efficiently at subsonic speeds. Furthermore, the need for future supersonic transport aircraft to conform to more stringent Stage 3 noise regulations[3] demands increased emphasis on minimising lift-dependent drag for take-off and climb conditions.

The large lift dependent drag of wings with leading-edge separation arises from the lack of suction forces on forward facing surfaces, resulting in low leading-edge thrust; thus, to obtain a factor closer to the theoretical ideal for planar wings, ie unity, it is necessary to re-establish this thrust. Figs 1a and b show two possible ways of achieving this aim; in

the first, the vortex flap (Fig 1a), the flow remains separated from the leading edge, but suctions induced on the forward-facing flap by the vortex sheet provide increased leading-edge thrust. In the second, 'attached-flow' approach (Fig 1b), an attempt is made to suppress leading-edge separation by a combination of a relatively-large leading-edge radius and nose camber. Again, the required thrust is obtained from suctions on forward-facing surfaces.

This paper is concerned mainly with the second type of flow. An area of special attention for this flow is the ordinary separation line on the part of the wing upper surface where the curvature is relatively large (Fig 1b). This separation is, generally, not obvious in surface pressure distributions. However, it can provoke leading-edge separation by acting as a route for boundary-layer air to migrate towards the outer wing[4]. The use of sub boundary-layer vortex generators to control this flow on a cambered delta wing is described in this paper. The emphasis is on understanding the flow control of the vortex generators rather than on their benefits, which have been considered previously[4].

Following a description of the experiment, the flows over the basic wing, ie without control, are discussed. The nature and effects of the control are described next and the paper ends with some concluding remarks.

Experimental details

Wind tunnel, model and measurements

The tests were performed at low speed in the 13ft x 9ft Wind Tunnel at the Defence Research Agency (DRA, formerly RAE) Bedford. This wind tunnel has an atmospheric working section, so that changes in wind speed lead to changes in both Mach number and Reynolds number. The wind tunnel has low turbulence levels; for example, at the wind speed of the present tests, 61m/s, turbulence levels in a working section reference plane are 0.014% in the longitudinal direction and 0.064% in the lateral direction.

The model was mounted on a mechanical balance located beneath the tunnel floor and comprised the port half of a wing-body configuration (Fig 2a). The wing has a leading-edge sweep of 60° and a Küchemann tip; streamwise sections were of 4% local thickness to chord ratio and have a leading-edge radius that was virtually constant across the span at 0.13% centre-line chord. The shape of the wing is illustrated in Fig 2b. The camber distribution was designed primarily to ensure satisfactory manoeuvre performance at supersonic speeds. However, it is expected that the camber would also improve manoeuvre performance at low speeds. The leading-edge droop angle in planes normal to the model axis was approximately 20° over most of the wing span.

Measurements were made of overall forces on the model using the underfloor balance, and static pressures were measured on the wing surface at a number of spanwise stations along the model axis (Fig 2a). There was a total of about 300 orifices, each of 0.5mm diameter and drilled normal to the surface. The orifices were mainly concentrated near the leading edge of the wing to allow accurate resolution of leading-edge thrust. The axial position of each of these stations is defined by x, the axial distance from the apex of the wing, made non-dimensional by the centre-line chord of the wing, c_0. The pressures were measured by electro-mechanical scanning of pressure transducers of range 34.5 kN/m^2. These measurements have been used to determine local and overall pressure forces on the wing and have also been used to infer the origin or point of onset of separation on the wing leading-edge. For this purpose, leading edge separation is assumed to take place at a given axial station when the minimum pressure coefficient at this station increases with angle of incidence, α. The angle of incidence at which this occurs defines the onset of leading-edge separation in the (x, α) plane.

The Vortex Generators (VG's) were in the form of thin wires of circular cross section, length 22.9mm ($0.0128c_0$) and of diameter d = 0.51mm ($0.00028c_0$). However, wires of smaller diameter, down to 0.13mm ($0.00007c_0$), were tested. Each wire was cut normal to its axis, pressed down on the wing surface and stuck with a contact adhesive. Fig 3 shows the geometry of the VG's on the wing upper surface. The position of a VG is defined by a particular axial station x_w, which the nose of the wire is downstream of by a fixed non-dimensional distance 0.0142, and the orientation by the angle between the axis of the VG and the wing leading edge in plan view, ϕ. Unless noted otherwise, the angle ϕ was 16.3°. The table in Fig 3 shows that multiple as well as single VG's were tested and defines the parameters varied. Three sets of multiple VG's were tested, the largest number, n = 56, being in Set 3; the other members of this set were obtained by successively removing every other VG, beginning with the most upstream VG.

Boundary-layer transition was allowed to occur naturally, owing to the difficulty of fixing transition near the leading edges of highly-swept wings. The VG's were always downstream of any laminar short bubbles and could therefore have influenced the bubbles only by altering the pressure distribution; however, the indications of pressure distributions were that any such effect was negligible.

No corrections have been made to the data for tunnel-wall constraint because the main aim of this study is to interpret the effect of VG's on the flows rather than to provide fully-corrected data. Repeatability of data between points within a test on a particular configuration was found to be ± 0.0002 for axial-force coefficient and ± 0.0015 for normal-force coefficient. Insufficient tests were made to assess the repeatability of the data between tests with nominally the same VG configuration, but a study of the data suggests that this is similar to that quoted above. Oil-flow studies were performed on the wing 'upper' surface for a selection of conditions using a mixture of diesel oil and pigment that was sensitive to ultra-violet light.

Test conditions

The wind speed of the tests, 61m/s, corresponds to a Mach number of 0.18 and a Reynolds number based on geometric mean chord of 3.9×10^6. This speed was chosen on the basis of a preliminary study[4]. This study showed that, for Reynolds

numbers above about 3 x 10^6, low Reynolds number effects associated with the bursting of the laminar bubbles are avoided and the changes of the flows with Reynolds number are much less pronounced than at low Reynolds number.

Basic wing flows

Fig 4 illustrates the change in character of the flow over the basic wing as angle of incidence increases by sketches of oil flows on the wing upper surface and two spanwise sections (AA and BB) of the stream-surfaces inferred from these oil flows.

Diagrams are shown for three angles of incidence: at the lowest angle of incidence, 11°, the ordinary separation line on the curved upper surface, S_1, is roughly parallel to the leading edge except near the wing root and intersects the trailing edge. Leading-edge separation S_2 occurs downstream of the point P on the leading edge at $x \simeq 0.87$, being due to the adverse pressure gradients and, perhaps, the high local sweeps of the isobars in the region of the Küchemann tip. This is referred to here as a 'locally-induced separation'. Separation of the returning flow beneath the vortex sheet is denoted by S_3. Upstream of P the leading-edge flow is attached, although there is evidence in the oil flows of a short bubble in this region at all the angles of incidence studied. This implies that the boundary layer of the flow approaching S_1 is turbulent. The reattachment lines corresponding to the separations S_1 and S_2 are referred to as R_1 and R_2.

At the next highest angle of incidence, 14°, the separation line S_1 intersects or joins the leading edge, implying that S_1 and S_2 are united and have a common reattachment line R, while the point P is further upstream than at $\alpha = 11°$. This type of leading-edge separation is referred to from here on as 'upstream- dependent'. The movement of the separation line S_1 towards the leading edge and the upstream movement of P between $\alpha = 11°$ and $\alpha = 14°$ are due to the increased severity of the adverse pressure gradients near the leading edge and the resulting increased migration of boundary layer air towards the wing tip as angle of incidence increases. At $\alpha = 16°$ the point P is still further upstream, and, at sufficiently high angle of incidence, $\alpha > 20°$, the flow at the leading edge becomes completely separated.

The effect of angle of incidence on the axial position of P (x_p) and the consequences of this are shown in Fig 5. Fig 5a shows that, for angles of incidence below about 11°, where locally-induced separation occurs near the tip, the axial position of point P changes only slowly with angle of incidence. However, at higher angles of incidence, where the leading-edge separation is upstream-dependent, the point P moves more rapidly with angle of incidence. Hence there is a marked increase in the rate at which lift-dependent drag factor $K = \pi A(C_D - C_{D0})/C_L^2$ increases with angle of incidence (Fig 5b). Also there is a noticeable pitch-up at an angle of incidence of about 14° (Fig 5c). This rapid forward movement of leading-edge separation with angle of incidence might have harmful consequences for lateral stability characteristics.

Thus the role of the ordinary separation line S_1 is of great significance and its effect on leading-edge separation may have unfavourable consequences. Therefore means of controlling this separation may be beneficial. In the next section this aspect is considered in some detail.

Nature and effects of control

Nature of control

The basic nature of the flow in the near region of a sub boundary-layer VG is illustrated by a sketch in Fig 6. Here the VG diameter is slightly larger than the (calculated) displacement thickness of the approaching boundary layer. A description of the near-field flow has been presented before[4] but is included here to aid the understanding of what follows. The main flow feature is the scarf vortex wrapped around the nose of the VG; this vortex is induced by the separation of the oncoming boundary layer and is a mechanism for converting boundary-layer vorticity (in the direction roughly normal to the external-flow direction) into streamwise vorticity. The axis of the VG is at an angle to the local flow direction; therefore the lee-side part of the scarf vortex, V, is the dominant flow feature, and it is this vortex that has the favourable effect on the boundary-layer flow. The direction of rotation of this vortex is such as to oppose the boundary-layer motion beneath it in the direction parallel to the separation line (section AA) and to increase the flow velocity near the wing surface towards the original separation line (section BB). The consequence is that the vortex causes a downstream displacement of the upper surface separation at a given spanwise position, leading, in turn, to a downstream shift of the point P.

It is reasonable to suggest that the strength of vortex V depends on the angle of the VG axis relative to the local flow direction and the VG height in relation to an appropriate boundary-layer thickness. These aspects are considered next.

Effects of control, single vortex generator

Effect of angle of incidence on control

Fig 7 summarises the effects of angle of incidence on the influence of a VG at $x_w = 0.45$ on the flow over the wing and the forces on the model. Fig 7a shows sketches of upper-surface oil flows at the same angles of incidence as for the basic wing (Fig 4). At the lowest angle of incidence 11°, the vortex V is weak and is of little consequence because the separation line S_1 does not intersect the leading edge, ie the leading-edge separation remains locally-induced. Thus the VG has no effect. At the higher angle of incidence, 14°, the leading-edge separation is upstream-dependent, as for the basic wing, and the vortex generator is effective in moving the point P downstream. At the highest of the three angles of incidence, 16°, the leading-edge separation is upstream-dependent, but the vortex V is weak compared with that at $\alpha = 14°$ and has little effect on the leading-edge flow. At this angle of incidence the nose of the VG is only just upstream of the separation line S_1. At angles of incidence above about 16.5° the VG is downstream of S_1 and consequently is unable to influence the position of P. This suggests that VG axial position and number are important parameters, and their effects are discussed later.

In Fig 7b the axial shift in P due to the VG is shown plotted against angle of incidence, and points corresponding to those in Fig 7a are marked on the plot, confirming the observations above. The curve has a maximum at an angle of incidence of about 14.5°. However, some further comments are needed to qualify this variation.

Two competing factors affect the downstream movement of P induced by the VG.

i) The strength of vortex V in the near region of vortex generator, which depends primarily on the mean speed of the flow approaching the VG and the angle between this mean flow vector and the axis of the VG. As angle of incidence increases, the speed of the flow at the outer edge of the boundary layer (the external flow) increases and the angle between the external-flow vector and the axis of the VG increases slowly. Both these effects are favourable. On the other hand, the twist within the boundary layer increases, reducing the angle between streamlines deep within the boundary layer and the axis of the VG. This explains why the VG loses its effectiveness as it approaches the separation line S_1. However, a further effect must be considered.

ii) The decay in the strength of the vortex between the vortex generator and the separation line, which depends on the distance between them[5]. Theoretical studies of two-dimensional flows, where skin friction coefficient and vortex height vary slowly with streamwise distance, show that the vortex decays exponentially with distance downstream[5,6]. Thus, from this point of view, the VG needs to be as close to the separation line as possible, although the increased twist in the boundary layer in this region may increase the rate of decay of the vortex[5]. As angle of incidence increases, the distance between the VG and the separation line S_1 decreases, which tends to increase the vortex strength at the separation line. Information given in Ref 5 and observations from the oil flows of the position of the separation line S_1, suggest that this is a significant, favourable effect, and that the unfavourable effect of twist in reducing vortex strength in the near field only becomes significant when the nose of the vortex generator is within a short distance of the separation line, perhaps of the order of a boundary-layer thickness. In this respect, it is interesting to note that the increase in the downstream shift of P due to the VG with angle of incidence is fairly gradual up to that for maximum shift, but, thereafter, this shift decreases rapidly. This is consistent with the nose of the VG entering the region of large twist close to the separation line.

The effects of the VG on normal and axial-force coefficients are shown in Fig 7c. In each case two sets of curves are included: i) overall forces from balance measurements, which have been shown to agree well with corresponding data inferred from pressure measurements[4], and ii) forces from integrations of pressure measurements between the wing root and the point P for the case with flow control. The latter is referred to as the 'attached-flow contribution' owing to the fact that, with control, the leading-edge flow on this part of the wing is attached.

At first sight, the changes in overall forces appear entirely consistent with the downstream shift in P. This reduction in the extent of leading-edge separation has the effect of reducing the 'non-linear' normal force associated with leading-edge vortex flows and of increasing leading-edge thrust. However, examination of the attached-flow contributions suggests that this is not a complete picture. At the angle of incidence for maximum reduction in normal force ($\alpha \simeq 15°$), most of the reduction is due to the attached-flow contribution. In contrast, for axial force, hardly any of the reduction comes from the attached-flow region, indicating, as noted before[4], that the increased leading-edge thrust comes from the reorganisation of the separated-flow region further downstream. The downstream movement of the origin of the leading-edge separation causes the leading-edge vortex to be closer to the forward-facing parts of the curved upper surface. The relative importance of these contributions for multiple VG's is considered later.

Effect of VG axial position

Figs 8a, b and c show the effect of VG axial position on the axial shift of P, normal-force coefficient and axial-force coefficient, respectively, for $\alpha = 14°$, 15° and 16°. For all three angles of incidence, there is a maximum value for the axial shift in P, the optimum position being at $x_w = 0.45$ for $\alpha = 14°$ and 15° and at $x_w = 0.39$ for $\alpha = 16°$.

There are two possible explanations for the decrease in effect as the VG is moved upstream of the optimum position. First, consider a VG with a vortex of given strength in the region of the separation line S_1. The controlling influence of the vortex on the boundary layer probably decreases with distance downstream. Thus, as the vortex generator is moved upstream from the optimum position, its effect on the boundary layer at a given position near the leading edge further downstream diminishes in comparison with that of local adverse pressure gradients. Secondly, the distance of the VG from the separation line increases until the VG is close to the wing root (as may be inferred from Fig 7a, $\alpha = 16°$), thus increasing the decay in vortex strength between the VG and the separation line. Hence, on this argument, the strength of V at the separation line (and hence its influence on the boundary-layer flow towards P) decreases as the VG moves upstream of the optimum position.

The loss in effectiveness of the VG as it is moved downstream of the optimum position can be explained in the same way as for the effect of angle of incidence. As the VG approaches the separation line S_1, the boundary-layer twist increases, and thus the mean angle between the approaching flow and the vortex generator axis decreases, with the further consequence that the strength of V declines. As noted before, once the VG is downstream of the separation line, it is no longer effective, and this explains why the VG position for zero effect moves upstream with increasing angle of incidence.

The variations of the normal-force and axial-force coefficients with axial position of the vortex generator (Figs 8b and c) generally correspond with the variation for the axial position of P.

Influence of VG angle

The effect of VG angle on the axial shift of P and increments in force coefficients is shown in Fig 9, where the various quantities are plotted against VG angle ϕ for α = 13°, 14°, 15° and 16° and for x_w = 0.45. The 'standard' angle 16.3° is close to the optimum in terms of either the axial shift of P (Fig 9a) or the reductions in normal force (Fig 9b) and axial force (or increase in leading-edge thrust) (Fig 9c) for the angles of incidence 14° and 15°. As the angle ϕ is increased above the optimum value, the axial shift of the point P and the force increments decrease until, by ϕ = 50°, they are negligible. Presumably, this loss of effectiveness occurs because the VG axis becomes aligned, in some mean sense, with the approaching boundary-layer flow. Hence, on this basis, the vortex generator is most effective at the angles of incidence 14° and 15° when its axis is at an angle of 34° to this mean flow direction. For the highest angle shown, α = 16°, the VG is almost ineffective at the 'standard' angle ϕ = 16.3°, a value of ϕ closer to zero giving a larger reduction in axial force than the 'standard' arrangement.

Fig 9 shows results inferred from calculations of the direction of the external flow and that limitingly close to the wing surface just upstream of the VG. The calculations were made using measured pressure distributions, together with the assumption that the flow near the leading edge was the same as that over an infinite yawed wing of the same leading-edge sweep. The boundary layer was calculated using an integral method for turbulent boundary layers[7], with boundary-layer transition inferred from oil-flow visualisations of the reattachment of the short bubble near the leading edge. The figures show calculated loci (for angles of incidence between 13° and 15°) corresponding to the VG being aligned with the external flow and with the flow limitingly close to the wing surface. The VG became ineffective at an angle which lies between the values given by these curves but which is closer to that for alignment with the external flow than that for alignment with the surface flow.

Effect of VG diameter

The influence of VG diameter on the axial shift of P and the increments in overall force coefficients is illustrated in Fig 10 for x_w = 0.45. The data are plotted in a similar way to that used for boundary-layer velocity profiles, with three ordinate scales, d/δ^*, $u_\tau d/\nu$ and d/c_0, where δ^* and u_τ are, respectively, calculated values of boundary-layer displacement thickness and wall friction velocity for an angle of incidence of 15°. The wall friction velocity is given by

$$u_\tau = \sqrt{(\tau_w / \rho)} \ ,$$

where τ_w is wall shear stress calculated by the integral boundary layer method referred to above. Fig 10 indicates that the change in the increments with VG diameter is small for values of d/δ^* between 0.6 and 1.2, but, for lower values, there is a rapid reduction in the increments with further decrease in diameter. By the value d/δ^* = 0.3, all three increments are almost zero, and it is significant that this corresponds roughly to $u_\tau d/\nu$ = 10, ie where the VG is almost wholly within the viscous sub layer[8]. This suggests that VG's which are submerged within this layer do not influence the flow over the wing.

Fig 10 also shows that the increments vary slowly with the parameter $u_\tau d/\nu$ for values between about 30 (ie approximately three times the maximum height of the viscous sub layer) and 60. This suggests that, for a given location of the separation line S_1 and a given value of d/c_0, the effects of Reynolds number on incremental force coefficients are unlikely to be significant for values of $u_\tau d/\nu$ in the range 30 to 60.

Effects of multiple vortex generators

As shown before[4], an increase in the number of VG's results in increasingly favourable control of the flow. However, interferences between the VG's may affect the performance of an array. Two radically-different types of interference are illustrated in Figs 11 and 12.

An adverse effect is illustrated schematically in Fig 11a and the consequences for the axial shift of the point P are shown in Fig 11b. This effect occurs when a single VG is upstream of the separation line S_1, so that it controls the flow towards P. When an additional VG is placed further upstream, the separation line is displaced away from the first VG (Fig 11a). Consequently, the vortex from the first VG has a larger distance over which to decay before reaching the separation line than previously and thus is not as effective as before. As further VG's are added upstream of the first, the adverse interference increases. The effect on the flow is illustrated in Fig 11b, which shows the axial shift of the point P for 1, 2 and 3 VG's compared with the corresponding values obtained by adding together the contributions of the individual VG's. As the number of VG's increases, so the reduction in effectiveness due to interference increases.

Fig 12 illustrates a favourable interference which occurs when a single VG is downstream of the separation line S_1 and is thus ineffective in controlling the flow towards P. The addition of a VG upstream of the first VG may cause the point P to move sufficiently far downstream so that the first VG then becomes effective (Fig 12a). The consequence is that the maximum value of angle of incidence for which the VG's remain effective increases. This is illustrated in Fig 12b. Owing to the difficulty of defining this angle of incidence from plots, such as sketched in the figure, an alternative definition is used which provides a measure of the increase in the upper limit of the range of effectiveness of the VG's. This angle, $\alpha_{1/2}$, is greater than that for maximum shift and corresponds to the angle where the shift is half the maximum value. The effect of increasing the number of VG's is to increase $\alpha_{1/2}$, although the rate at which it increases with VG number drops noticeably above 28 VG's.

Increasing the number of VG's generally has an increasingly favourable effect on the downstream movement of P and the increase in leading-edge thrust. This is illustrated in Fig 13, which shows the variation of axial shift of P and axial and normal-force coefficients with VG number for α = 15°, 16° and 17°. As the number of VG's in Set 3 increases up to 28 for a given angle of incidence, the length of leading edge

over which the flow is attached increases and leading-edge thrust increases. However, with further increase of VG number to 56, the effects are less favourable.

As an aid to understanding these observations, Fig 14 shows photographs of surface oil flows, spanwise pressure distributions and cross-sections through stream surfaces at x = 0.87 (inferred from the oil flows and pressure distributions) for three configurations with 7, 28 and 56 VG's at $\alpha = 15°$. For this axial station the leading-edge flow is separated. With 7 VG's, the separation line S_1 joins the leading edge, so that the leading-edge separation becomes upstream dependent. In contrast, for 28 VG's, S_1 intersects the trailing edge and thus the leading-edge separation becomes locally-induced. This implies a limit to the control that is available from vortex generators, since their effect on the leading-edge flow is no longer direct. Consequently, in this circumstance, leading-edge separation in this region can only be prevented by increasing the leading-edge droop. The spanwise pressure distributions show that much higher suctions are attained near the leading edge with 28 VG's than with 7 VG's, and this is consistent with the point P moving downstream as the number of VG's increases from 7 to 28.

The flow for 56 VG's is complex. Although only one reattachment line is indicated by the oil flow, both the pressure distributions and oil flows suggest two concentrated regions of vorticity in the flow above the wing. This implies that the two separations S_1 and S_2 become united in a complex way to give the single vortex sheet with two cores as suggested in the sketch. The leading-edge separation in this flow is therefore upstream dependent and the result is that the point P is further upstream than for 28 VG's. This is reflected in the suctions near the leading edge being lower for 56 than for 28 VG's. The loss of performance between 28 and 56 VG's appears to be due to increased interference between the vortices as the VG's become closer together. Viscous interactions between closely-spaced vortices have been found to increase their streamwise rate of decay[5]. Insets in the figure show close-up photographs of the oil flows in the region of the VG's, illustrating the complexity of the interactions between the vortices for configurations with relatively-large numbers of VG's.

Fig 15 shows a similar presentation for $\alpha = 17°$. For 7 VG's only two or possibly three VG's appear to be effective, and the separation line S_1 intersects the leading edge at $x \simeq 0.45$. With 28 VG's the flow is similar to that for 56 VG's at $\alpha = 15°$, ie only one reattachment line intersects the trailing edge but there are two regions of concentrated vorticity in the separated vortex sheet. In some respects the flows for 28 and 56 VG's at $\alpha = 17°$ are similar in that only one attachment line intersects the trailing edge in either case; however the oil flows suggest a marked change in the character of the oil flow between 28 and 56 VG's. In addition, there were indications from the overall-force measurements that the flow with 56 VG's was unsteady, possibly because the flow switched from one state to another.

In the discussion of Fig 7 the relative contributions to incremental forces of the attached and separated parts of the flow were considered for a single VG. Figs 16a and b show the variation of the ratio (attached-flow contribution to force coefficient)/(overall-force coefficient) with VG number for normal and axial forces, respectively. For normal force, as VG number increases, the relative contribution of the attached-flow part becomes larger. For axial force (Fig 16b) the attached-flow contribution reaches a maximum for a VG number between 28 and 56. This maximum value depends on angle of incidence but is about 0.6 at $\alpha = 15°$. This shows that the reorganisation of the flow in the region where the leading-edge flow is separated remains an important effect even for a large number of VG's. Further evidence of this effect is found in Figs 14 and 15 where the suctions on the forward-facing surfaces in the separated-flow region are shown to be significantly larger for 28 VG's than for 7 VG's.

It is interesting to consider the influence of the most efficient arrangement of multiple VG's tested (28) on the parameters previously shown plotted against angle of incidence or lift coefficient for the basic wing in Fig 5. The revised presentation is shown in Fig 17. The favourable effect of the VG's in extending the range of angles of incidence over which the leading edge flow is not directly influenced by boundary-layer conditions upstream (locally-induced separation) is shown in Fig 17a. The angle of incidence at which the leading edge separation changes to upstream dependent is increased from about 11° to 17.5°. The consequence is that the range of angles of incidence over which the upstream movement of P with angle of incidence is gradual is increased. Further consequences are that the VG's reduce lift-dependent drag factor by about 16% at a lift coefficient of 0.6 (Fig 17b) and increase the lift coefficient where pitch-up occurs by about 0.1. Thus, by controlling leading-edge separation, multiple, miniature VG's offer significant aerodynamic benefits for highly-swept cambered wings.

Although no wing buffeting measurements were made during these tests, previous experiments on wings with these types of flow[9] suggest that the VG's would delay buffet onset a little and raise the light buffeting level significantly. However, the moderate and heavy buffeting levels would probably be unaffected.

Concluding remarks

This paper describes the control of leading-edge separation on a cambered delta wing by small (sub boundary-layer) vortex generators placed close to the leading edge on the wing upper surface. The effectiveness of the vortex generators is judged primarily by the amount by which they increase the length of attached flow at the leading edge. This effectiveness depends on a number of factors:

i) Where the VG is in relation to an ordinary separation line on the curved upper surface If the VG is downstream of the ordinary separation line, it cannot affect the boundary-layer flow towards the origin of the leading-edge separation. Thus VG's must be upstream of the ordinary separation line if they are to control leading edge separation. The optimum performance of a VG occurs when it is close to this separation line, the benefit diminishing as the VG moves further upstream.

ii) Whether or not the ordinary separation intersects the leading edge Only if this separation intersects the leading edge can the VG's affect the leading-edge separation directly. Otherwise, leading edge separation is locally induced, and then other devices, such as increased leading-edge droop, become necessary to prevent or to minimise leading-edge separation in this region.

iii) The angle between the VG axis and the leading edge
For angles of incidence between 13° and 15°, the optimum angle for a single VG is about 16°, independent of axial position of the VG.

iv) The height of the VG The variation of the effect of the VG on the flow with height is small so long as the parameter $u_\tau d/\nu$ is in the range 30 to 60 (ie the VG height is between roughly three times and six times the maximum height of the viscous sub-layer).

v) Number of VG's Generally, an increase in the number of VG's has beneficial effects, although there can be unfavourable interferences between VG's. One favourable effect is an increase in the range of angle of incidence over which the VG's are effective with VG number. Unfavourable effects include:

a) the movement of the ordinary separation line away from a VG due to the action of a VG further upstream, with the result that the vortex of the first VG is of lower strength at the separation line owing to the effect of viscous decay, and

b) destructive interference between vortices of VG's placed too close together.

The optimum number of VG's found in the present study, in terms of increased leading-edge thrust, was 28. Compared to the basic wing, the lift-dependent drag factor is lower by about 16% at a lift coefficient of 0.6 and the pitch up associated with the rapid movement of the leading-edge separation with angle of incidence is delayed by a lift coefficient of approximately 0.1 for this number of VG's.

Thus, in conclusion, miniature vortex generators can have a significant controlling influence over the leading-edge separations on cambered wings with highly-swept leading edges. These devices are likely to be beneficial both to future combat aircraft and advanced supersonic transport aircraft.

Acknowledgements

The authors would like to thank Mrs N Rycroft for her efforts in preparing the diagrams.

References

1 Küchemann, D., "The Aerodynamic Design of Aircraft." Pergamon Press Ltd, Oxford, 1978.

2 Küchemann, D., "Flows with separations." RAE TM Aero 453,1955.

3 Piellisch, Richard, "Mach 2 and above." Aerospace America, January 1994, pp 17-19&31.

4 Ashill, P. R. and Riddle, G. L., "Control of leading-edge separation on a cambered delta wing." Paper No. 11, AGARD-CP-548, October 1993.

5 "Vortex generators for control of shock-induced separation Part 1: Introduction and aerodynamics." ESDU Transonic Data Memorandum 93024, December 1993.

6 Wendt, B. J., Greber, I. and Hingst, W.R., "The structure and development of streamwise vortex arrays embedded in a turbulent boundary layer." NASA Tech Memo 105211, 1991.

7 Ashill, P. R. and Smith, P. D., "An integral method for calculating the effects on turbulent boundary-layer development of sweep and taper." The Aeronautical Journal, February 1985, pp 43-54.

8 Young, A. D., "Boundary Layers." BSP Professional Books, Oxford, 1989.

9 Mabey, D. G., "A review of scale effects in unsteady aerodynamics." Prog. Aerospace Sci, Vol 28,1991, pp 273-321.

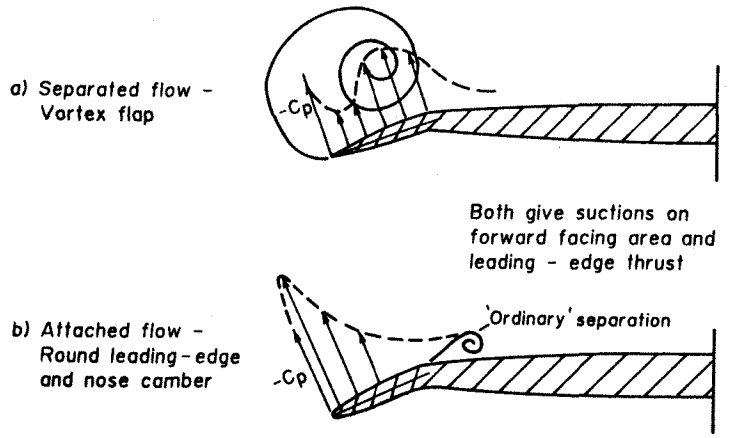

Fig 1 Two methods for providing increased leading-edge thrust.

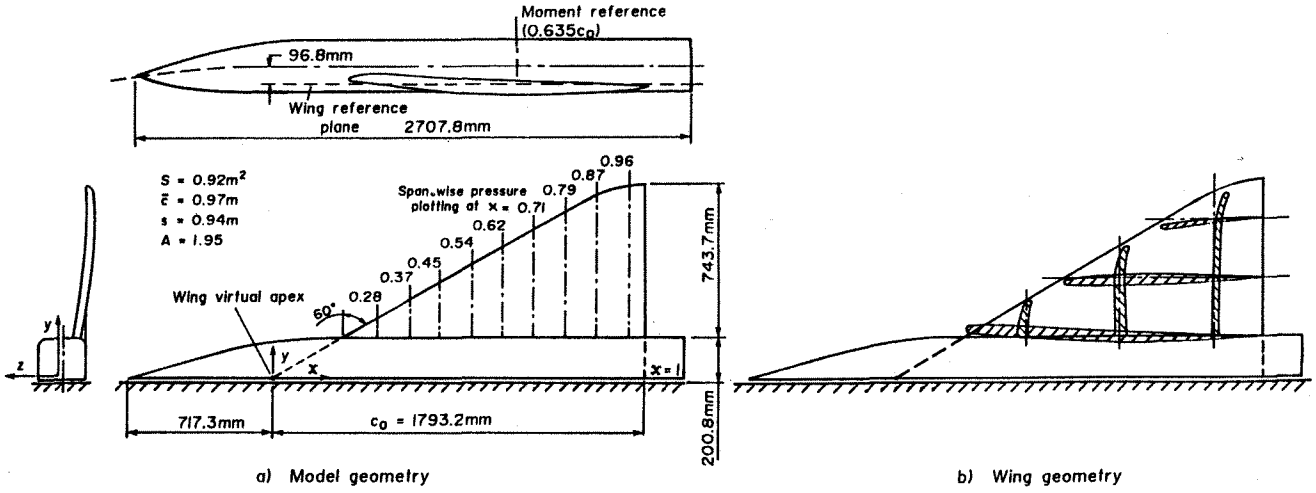

Fig 2 Model and wing geometry.

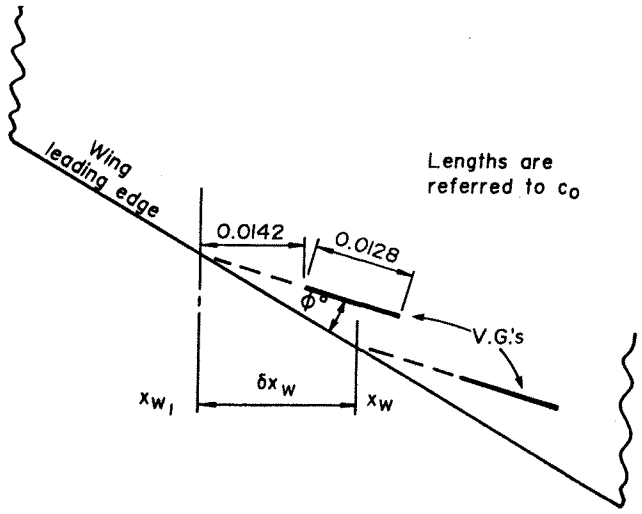

n	x_{w1}	δx_w	set
2	0.368	0.0843	1
3	0.284	0.0843	2
7	0.284	0.0843	
14	0.241	0.0422	3
28	0.220	0.0211	
56	0.209	0.0105	

Fig 3 Vortex generator geometry.

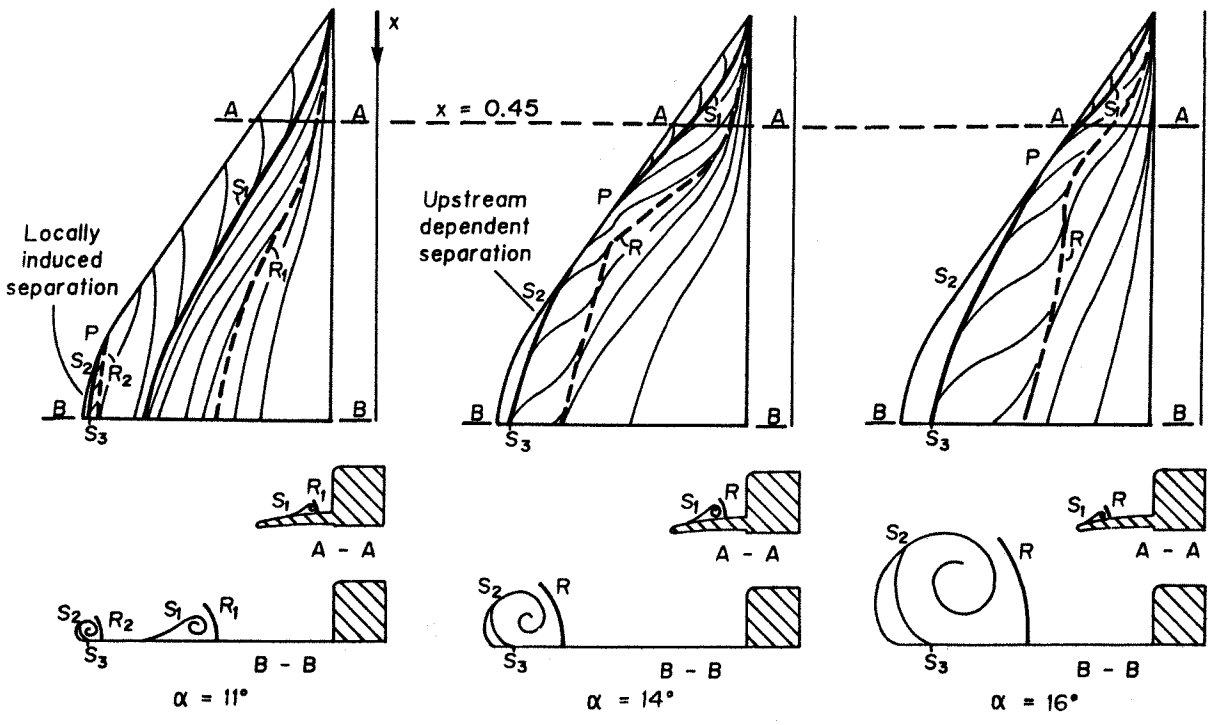

Fig 4 Flows over basic wing.

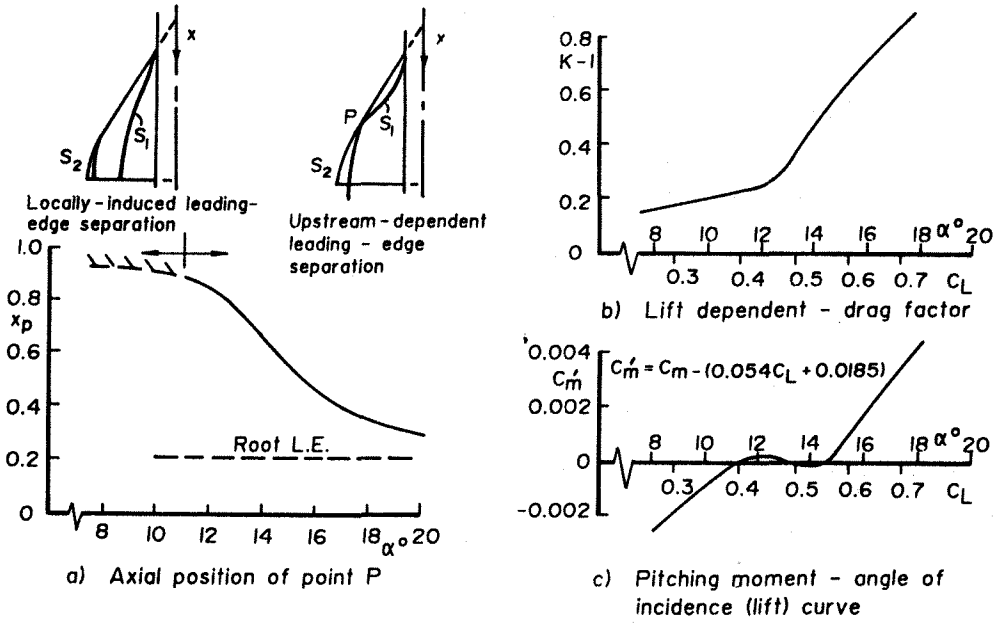

Fig 5 Effect of angle of incidence on axial position of point P, lift-dependent drag factor and pitching-moment coefficient.

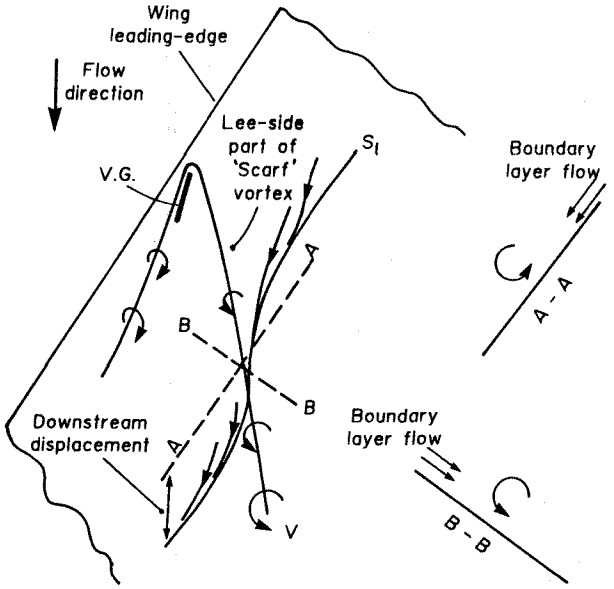

Fig 6 Flow in near region of vortex generator.

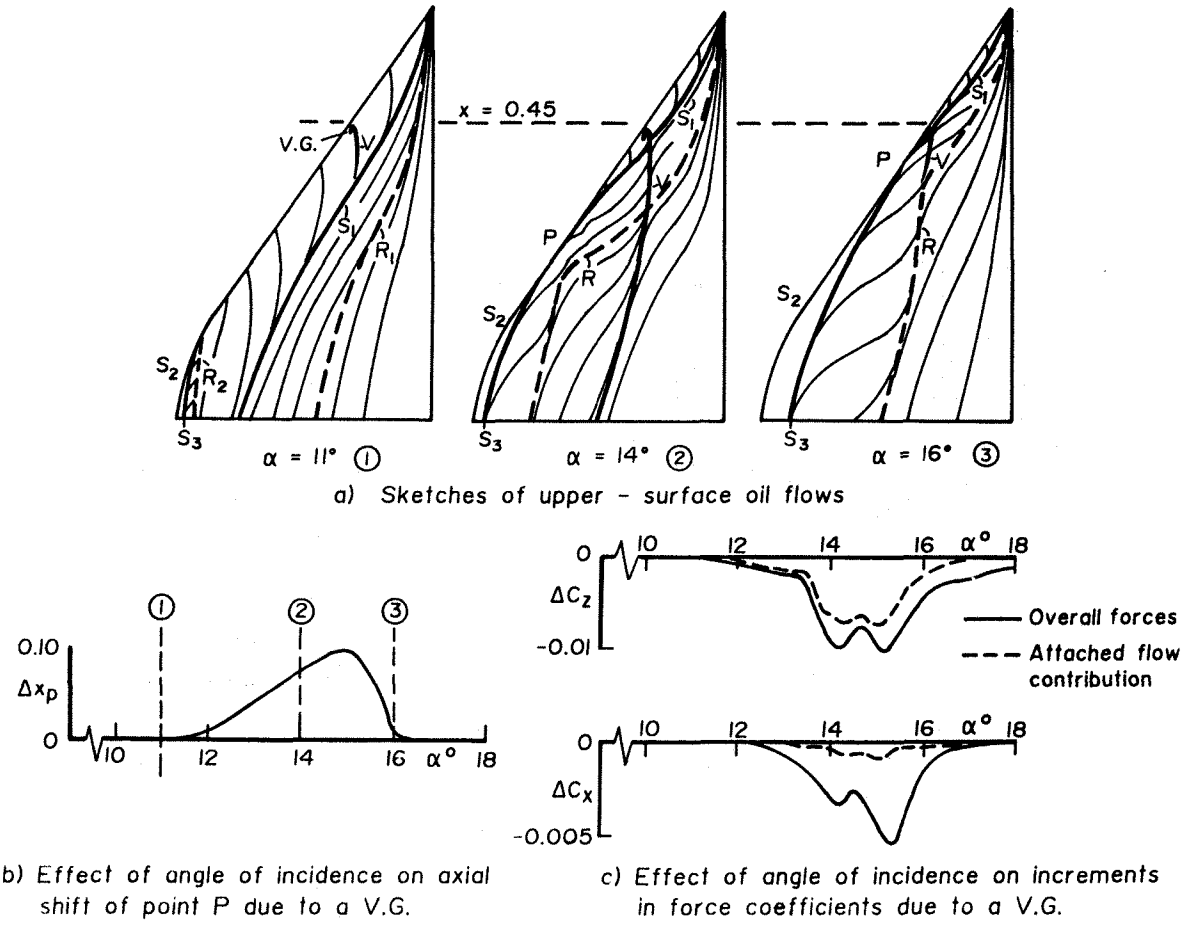

Fig 7 Effects of angle of incidence on the effect of a vortex generator at $x_w = 0.45$ on flow over wing and forces on model.

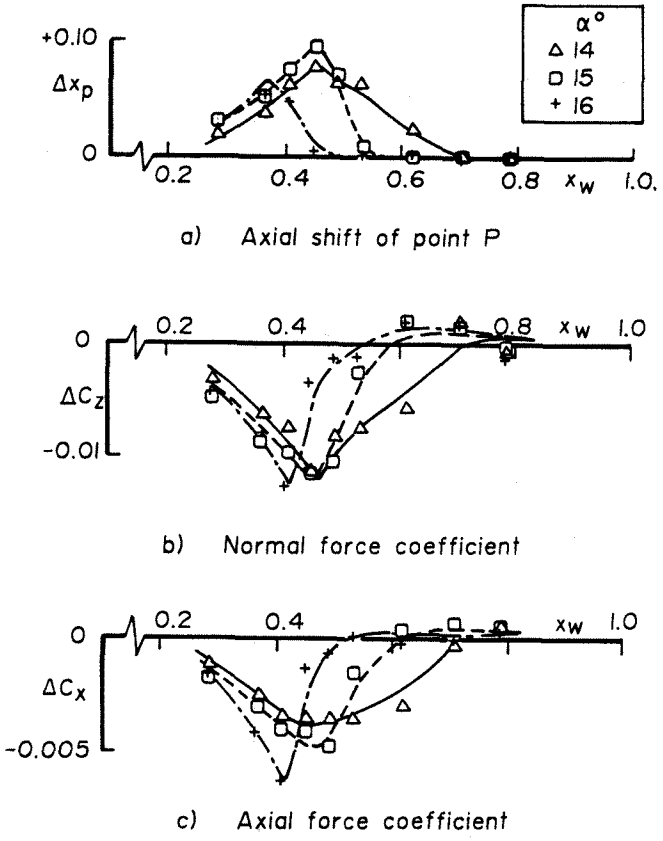

Fig 8 Effect of VG axial position on axial shift of point P, normal-force coefficient and axial-force coefficient.

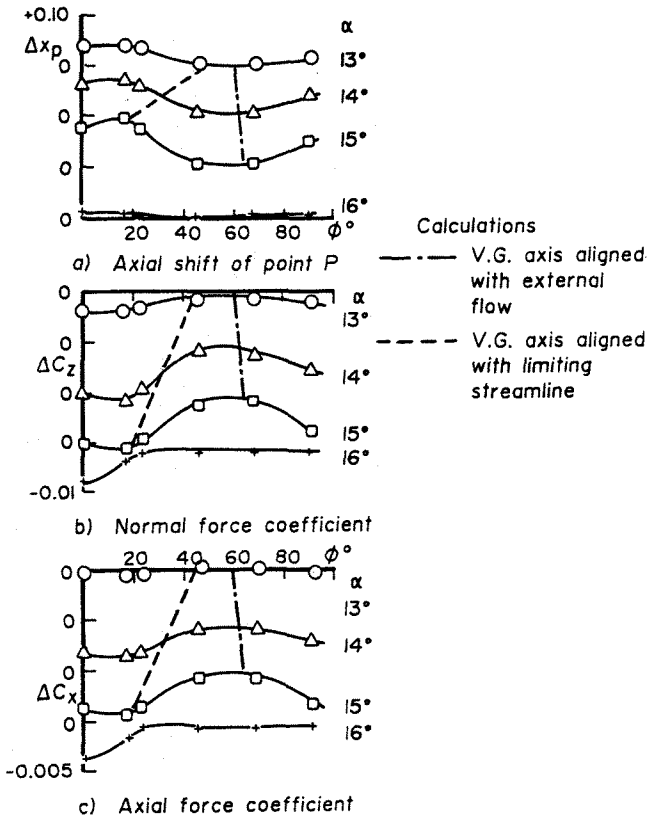

Fig 9 Effect of VG angle, ϕ, on axial shift of point P, normal-force coefficient and axial-force coefficient.

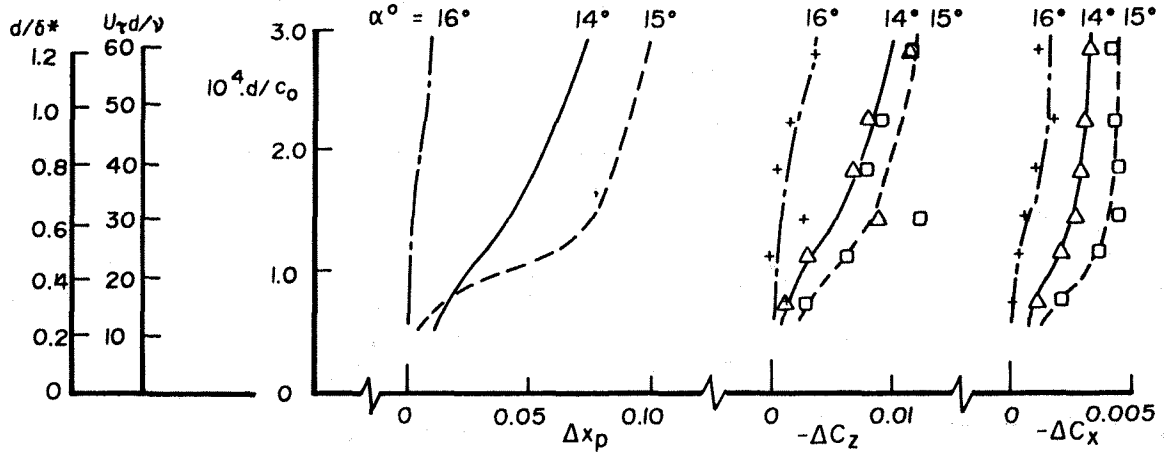

Fig 10 Effect of VG diameter on axial shift of point P, normal-force coefficient and axial-force coefficient, $x_w = 0.45$.

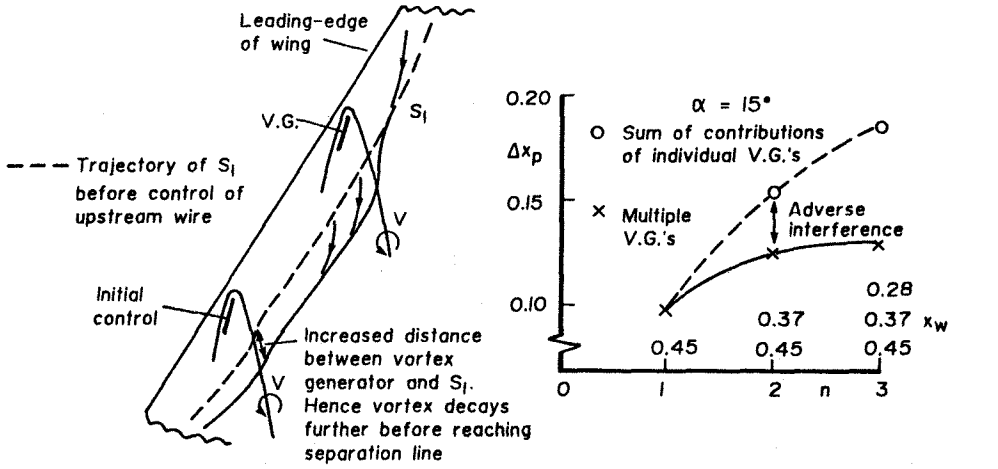

a) Sketch illustrating adverse interference of one V.G. on another

b) Consequence of adverse interference for axial shift of point P

Fig 11 Adverse interference between vortex generators.

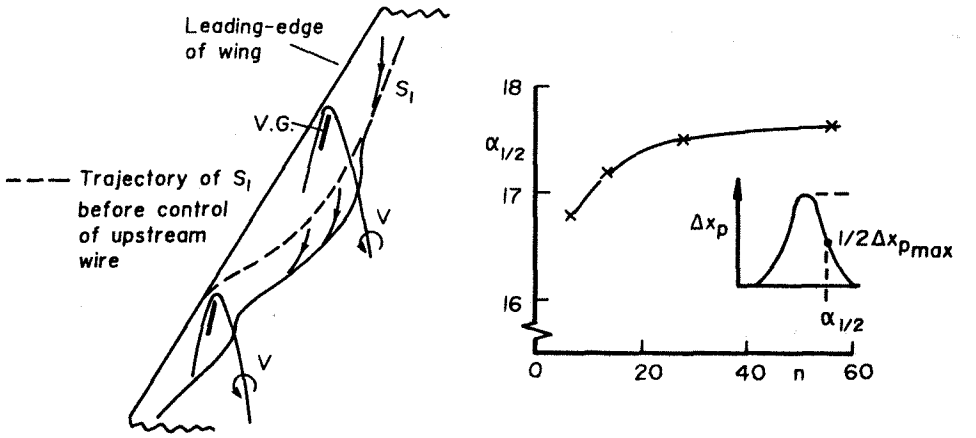

a) Sketch illustrating favourable interference between V.G.'s

b) Consequence of favourable interference for range of angles of incidence over which V.G.'s are effective

Fig 12 Favourable interference between vortex generators.

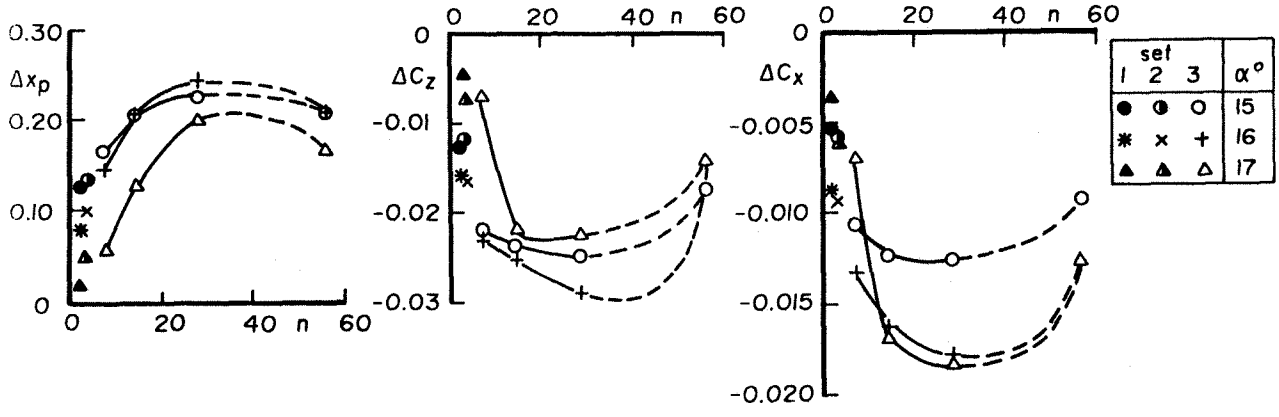

a) Axial position of point P

b) Normal force coefficient

c) Axial force coefficient

Fig 13 Effect of vortex generator number on axial shift of point P, normal-force coefficient and axial-force coefficient.

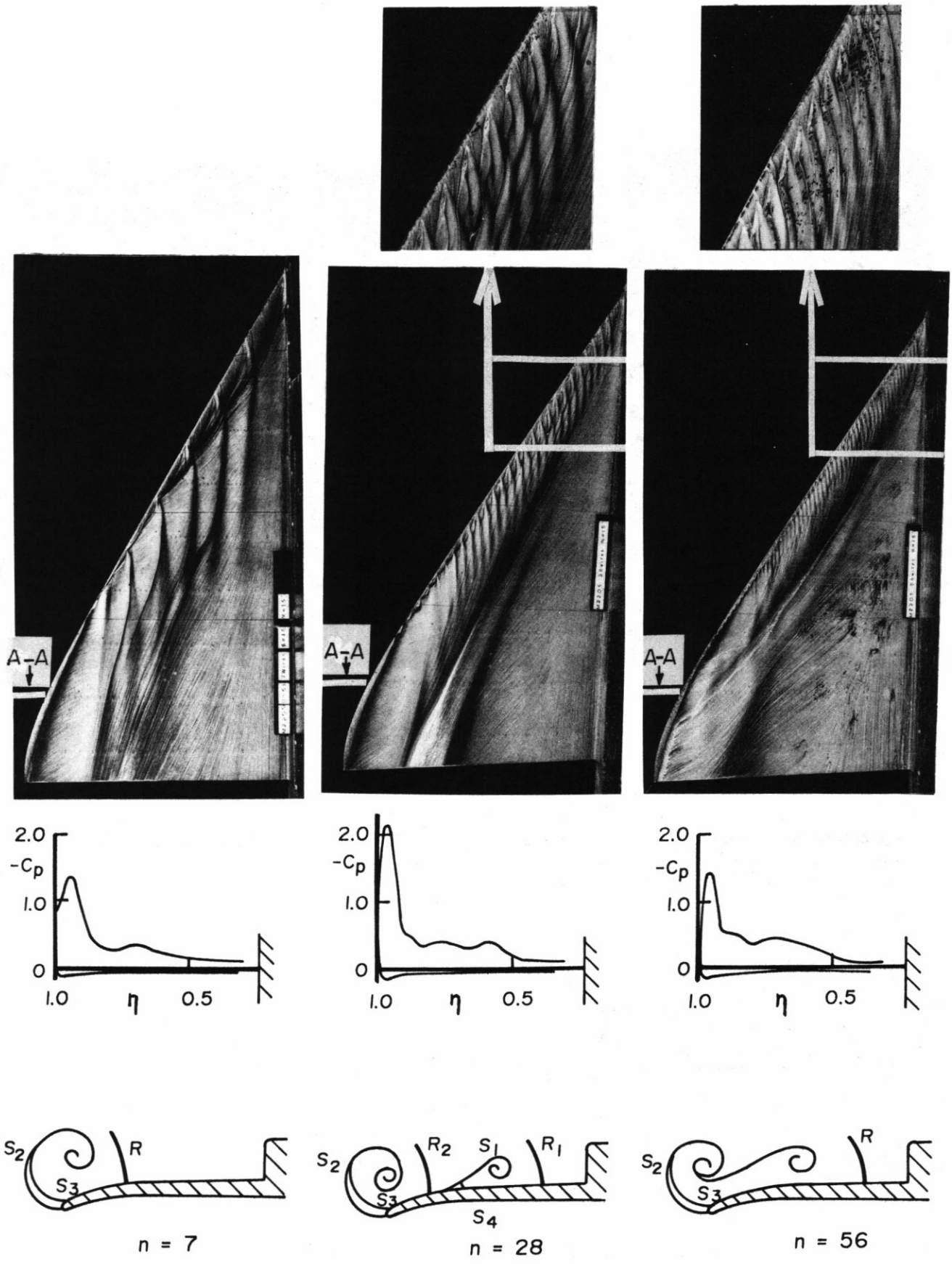

Fig 14 Measured and inferred flows for three different VG numbers, $\alpha = 15°$ (Section AA, x = 0.87).

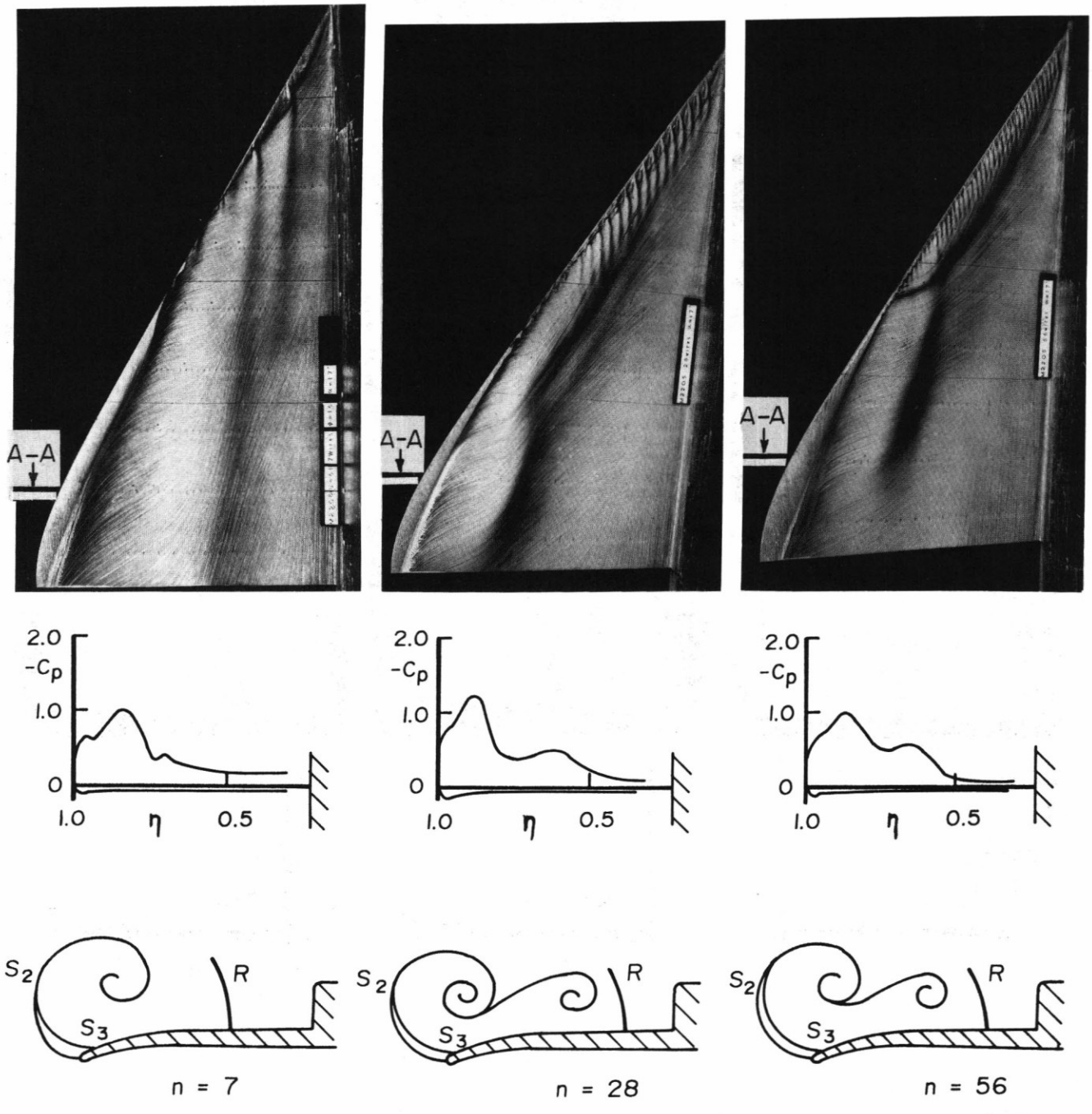

Fig 15 Measured and inferred flows for three different VG numbers, $\alpha = 17°$ (Section AA, x = 0.87).

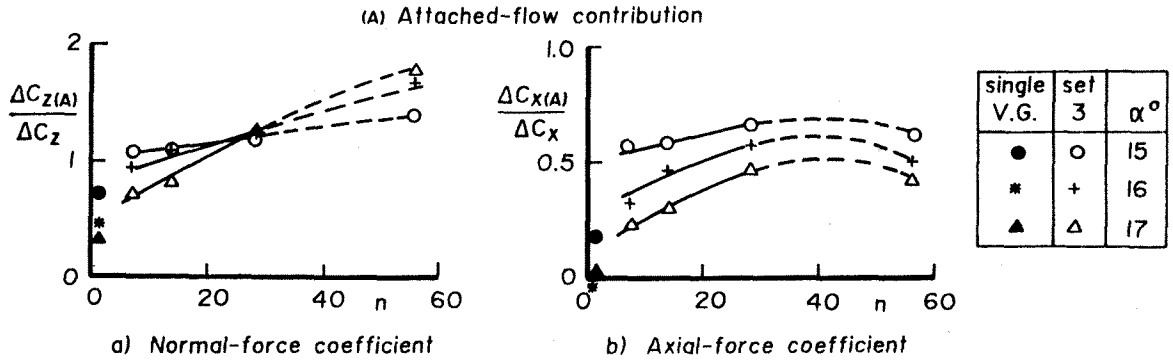

Fig 16 Effect of VG number on ratio of attached flow contribution to force to overall force.

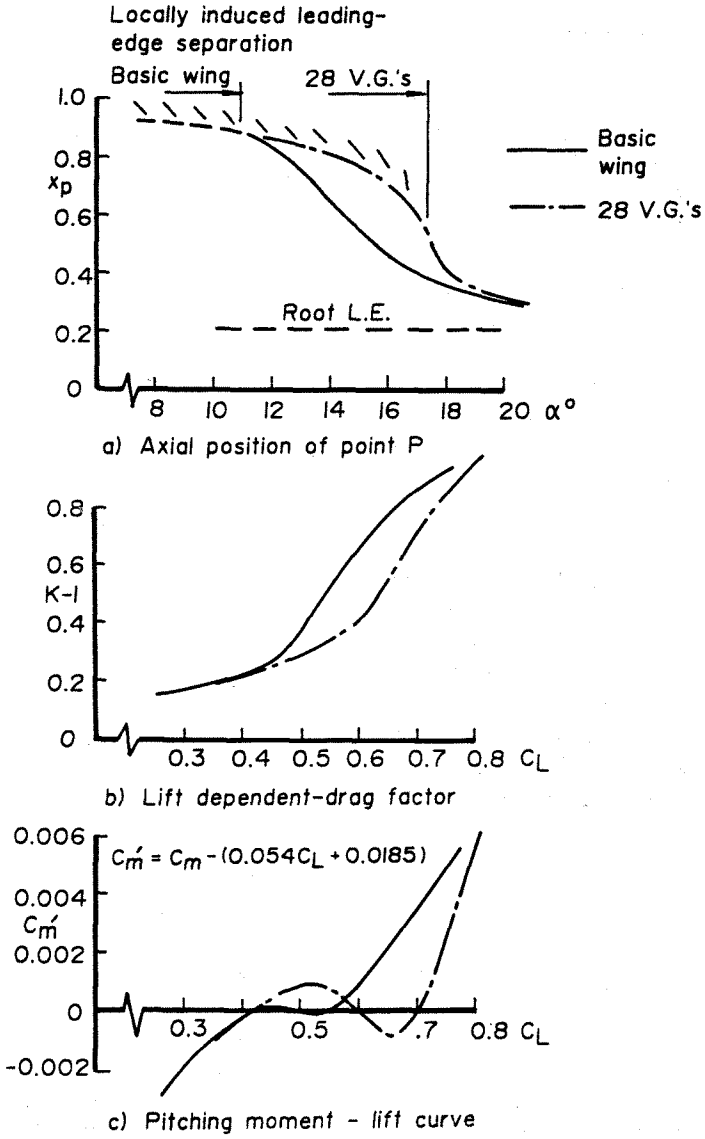

Fig 17 Effect of angle of incidence or lift coefficient on axial position of point P, lift-dependent drag factor and pitching-moment coefficient.